

Numerical Verification of Fluctuation Dissipation Theorem for Isolated Quantum Systems

Jae Dong Noh,¹ Takahiro Sagawa,² and Joonhyun Yeo³

¹*Department of Physics, University of Seoul, Seoul 02504, Korea*

²*Department of Applied Physics, The University of Tokyo,
7-3-1 Hongo, Byunkyo-ku, Tokyo 113-8656, Japan*

³*Department of Physics, Konkuk University, Seoul 05029, Korea*

(Dated: July 16, 2020)

The fluctuation dissipation theorem (FDT) is a hallmark of thermal equilibrium systems in the Gibbs state. We address the question whether the FDT is obeyed by isolated quantum systems in an energy eigenstate. In the framework of the eigenstate thermalization hypothesis, we derive the formal expression for two-time correlation functions in the energy eigenstates or in the diagonal ensemble. They satisfy the Kubo-Martin-Schwinger condition, which is the sufficient and necessary condition for the FDT, in the infinite system size limit. We also obtain the finite size correction to the FDT for finite-sized systems. With extensive numerical works for the XXZ spin chain model, we confirm our theory for the FDT and the finite size correction. Our results can serve as a guide line for an experimental study of the FDT on a finite-sized system.

Introduction— It is a fascinating question to ask when and how isolated quantum many body systems approach the thermal equilibrium state. Recent advances in experimental techniques with ultracold atoms boost research interests, theoretical and experimental, in quantum thermalization [1–6]. The relaxation of an isolated quantum system into a stationary state has been proved in a broad range of systems and initial states [7–10]. Thermalization furthermore requires that this stationary state is indistinguishable from the equilibrium microcanonical state.

It is the eigenstate thermalization hypothesis (ETH) that makes a link between the stationary state and the Gibbs state. The ETH is an assumption for matrix elements of local observables in the Hamiltonian eigenstate basis [11–13]. Under the ETH, expectation values of observables in the Hamiltonian eigenstates coincide with the microcanonical ensemble averages. The ETH has been tested extensively, and is believed to hold in non-integrable systems [14–16]. It is confirmed that matrix elements of observables display the statistical properties postulated by the ETH [17–21]. Thermalization after quantum quench [22, 23] and thermodynamic processes such as the Joule expansion are also understood well in the framework of the ETH [24, 25].

The fluctuation dissipation theorem (FDT), which provides the universal relation between the response (or dissipation) and the correlation (or fluctuation), is another hallmark of thermal equilibrium states [26, 27]. As equilibrium dynamics is characterized by the detailed balance, the dynamic response function and the correlation function of equilibrium systems are not independent but tightly linked to each other. The FDT has been used to distinguish equilibrium and nonequilibrium dynamics [28] and to measure the temperature of microscopic quantum systems [29, 30].

There have been growing number of studies on the connection between the quantum thermalization and the

fluctuation and dissipation in isolated quantum systems. Foini *et al.* [31, 32] investigated the relaxation dynamics of an integrable quantum system which is nonthermal. Essler *et al.* [33] proposed an argument connecting static and dynamic correlations based on the Lieb-Robinson bound [34]. Srednicki [35] studied a version of FDT for isolated quantum systems which involves the correlation of the *expectation values* of observables. This in fact corresponds to the classical limit of the full quantum mechanical FDT and has been further investigated in Refs. [36, 37]. D’Alessio *et al.* [12] demonstrated that the FDT with a single observable is consistent with the ETH. The FDT with two different observables requires an assumption on the behavior of the random variables arising in the ETH, which needs to be verified.

In this Letter, we present an explicit numerical verification and a comprehensive study of the FDT in isolated quantum systems. In the framework of the ETH, we derive a symmetry relation among the quantum mechanical two-time correlation functions, known as the Kubo-Martin-Schwinger (KMS) condition [27, 38]. Combining the symmetry relation and the linear response theory, we show that an isolated quantum system in an energy eigenstate obeys the FDT in the *infinite size limit*. Finite-sized systems violate the FDT. We derive the analytic expression for the *finite size correction* to the FDT. When the energy uncertainty or variance of the quantum state scales as $\Delta^2 E = O(L^d)$ or is smaller than that, the finite size correction term scales as $O(L^{-d})$ with the system size L and the spatial dimension d . We verify our analytic theory with the exact diagonalization study for the XXZ spin chain, equivalently the hardcore boson model, in one-dimensional lattices. We demonstrate the finite size correction to the FDT using the energy eigenstate.

KMS Condition and FDT— A quantum system with Hamiltonian \hat{H} is in an initial state $\hat{\rho}_i$ at time $t = t_0$. When a perturbation $\delta\hat{H} = -h(t)\hat{B}$ is applied, an ex-

pectation value of an observable \hat{A} at time $t > t_0$ deviates from its unperturbed value. According to the linear response theory [27, 39], the deviation is given by $\delta A(t) = 2i \int_{t_0}^t dt' \chi''_{AB}(t, t') h(t') + O(\hbar^2)$ with the linear response function

$$\begin{aligned} \chi''_{AB}(t, t') &\equiv \frac{1}{2\hbar} \langle [\hat{A}(t), \hat{B}(t')] \rangle_i \\ &= \frac{1}{2\hbar} (\bar{S}_{AB}(t, t') - \bar{S}_{BA}(t', t)). \end{aligned} \quad (1)$$

The operators are in the Heisenberg picture with respect to the unperturbed Hamiltonian, $\langle \rangle_i$ stands for the expectation value in the state $\hat{\rho}_i$, and $\bar{S}_{AB}(t, t') \equiv \langle \hat{A}(t) \hat{B}(t') \rangle_i - \langle \hat{A}(t) \rangle_i \langle \hat{B}(t') \rangle_i$ is the two-time connected correlation function. The response function is defined for both $t \geq t'$ and $t < t'$. The causal response function is given by $\chi_{AB}(t, t') = 2i\Theta(t - t')\chi''_{AB}(t, t')$ with the Heaviside step function $\Theta(t - t')$.

Suppose that the system is prepared in the thermal equilibrium state characterized by the Gibbs state $\hat{\rho}_i = \hat{\rho}_{eq}(\beta) = e^{-\beta\hat{H}}/Z$ with inverse temperature β and the partition function Z . Throughout the paper, we set the Boltzmann constant $k_B = 1$. The equilibrium state is stationary so that the correlation function and the response function depend on the time difference $t - t'$. Furthermore, since the Boltzmann factor $e^{-\beta\hat{H}}$ is equal to the time evolution operator in the imaginary time direction, the correlation functions obey the KMS condition [27, 38] that

$$\bar{S}_{AB,eq}(t) = \bar{S}_{BA,eq}(-t - i\beta\hbar) \quad (2)$$

or, equivalently,

$$\bar{S}_{AB,eq}(\omega) = \bar{S}_{BA,eq}(-\omega) e^{\beta\hbar\omega} \quad (3)$$

in the frequency domain. A Fourier transformation is defined by $\bar{S}_{AB,eq}(\omega) = \int_{-\infty}^{\infty} dt \bar{S}_{AB,eq}(t) e^{i\omega t}$. Combining the KMS condition and the linear response theory, one obtains the celebrated quantum mechanical *fluctuation dissipation theorem*

$$\chi''_{AB,eq}(\omega) = \frac{1 - e^{-\beta\hbar\omega}}{2\hbar} \bar{S}_{AB,eq}(\omega). \quad (4)$$

In the classical limit where $\hbar \rightarrow 0$, it becomes

$$\bar{S}_{AB,eq,cl}(\omega) = \frac{2}{\beta\omega} \chi''_{AB,eq,cl}(\omega). \quad (5)$$

Integrating over all ω , one obtains the familiar relation

$$\chi_{AB,eq,cl}(\omega = 0) = \beta \bar{S}_{AB,eq,cl}(t = 0) \quad (6)$$

between the static susceptibility and the equal time correlation function [27]. We stress that the KMS condition in Eq. (2) or (3) is the necessary and sufficient condition for the FDT in Eq. (4) provided that the linear response theory is valid.

FDT from ETH— We address the question whether the FDT holds for a generic nonintegrable quantum system not necessarily in the Gibbs state. In the framework of the ETH, we formulate the FDT with a focus on the KMS condition. Note that the KMS condition can be examined numerically easily, as will be shown later. We will denote Hamiltonian eigenstates and eigenvalues as $\{|\alpha\rangle\}$ and $\{E_\alpha\}$.

Suppose that the initial state is given by $\hat{\rho}_i = \sum_\alpha p_\alpha |\alpha\rangle\langle\alpha|$. The mean energy and the energy variance are given by $\bar{E} = \langle \hat{H} \rangle_i$ and $\Delta^2 E = \langle (\hat{H} - \bar{E})^2 \rangle_i$. Such a state is called the diagonal ensemble which corresponds to the stationary state limit of a pure state $|\psi\rangle = \sum_\alpha c_\alpha |\alpha\rangle$ with $p_\alpha = |c_\alpha|^2$ [14]. An energy eigenstate $|\alpha_0\rangle\langle\alpha_0|$ is a special case with $p_\alpha = \delta_{\alpha\alpha_0}$. The inverse temperature β of the initial state is determined by $\bar{E} = \text{Tr } \hat{H} \hat{\rho}_{eq}(\beta)$. Let \hat{A} and \hat{B} be Hermitian operators for observables. The correlation function $\bar{S}_{AB}(\omega)$ for $\omega \neq 0$ is given by

$$\bar{S}_{AB}(\omega) = 2\pi \sum_\alpha \sum_{\gamma \neq \alpha} p_\alpha A_{\alpha\gamma} B_{\gamma\alpha} \delta(\omega - \omega_{\gamma\alpha}) \quad (7)$$

with $\omega_{\gamma\alpha} \equiv (E_\gamma - E_\alpha)/\hbar$ and $A_{\alpha\gamma} = \langle \alpha | \hat{A} | \gamma \rangle$, etc.. If the initial state is the equilibrium Gibbs state $\hat{\rho}_{eq}(\beta)$, each term in \bar{S}_{AB} and \bar{S}_{BA} has the ratio $p_\alpha/p_\gamma = e^{\beta\hbar\omega_{\gamma\alpha}}$. Thus, the KMS condition (3) holds identically regardless of characteristics of the operators. For nonthermal states, however, the KMS condition requires a specific property of the operators.

According to the ETH, matrix elements of a Hermitian operator \hat{X} in the energy eigenstate basis has the structure

$$X_{\gamma\alpha} = X(E_{\gamma\alpha}) \delta_{\gamma\alpha} + e^{-S(E_{\gamma\alpha})/2} f_X(E_{\gamma\alpha}, \omega_{\gamma\alpha}) R_{\gamma\alpha}^X, \quad (8)$$

where $E_{\gamma\alpha} = (E_\gamma + E_\alpha)/2$, $\omega_{\gamma\alpha} = (E_\gamma - E_\alpha)/\hbar$, $S(E)$ is the microcanonical ensemble entropy, R^X is a random matrix in the Gaussian unitary ensemble, and $X(E)$ and $f_X(E, \omega) = f_X(E, -\omega)^*$ are smooth functions [11, 12]. Using (8) for \hat{A} and \hat{B} , it is straightforward to obtain that [40]

$$\begin{aligned} \bar{S}_{AB}(\omega) &= 2\pi \exp \left[\frac{1}{2} \beta \hbar \omega + \mathcal{Y}_{AB}(\bar{E}, \omega) \right] \\ &\quad \times f_A(\bar{E}, -\omega) f_B(E, \omega) \mathcal{R}_{AB}(\bar{E}, \omega), \end{aligned} \quad (9)$$

where $\mathcal{R}_{AB}(E, \omega)$, called an overlap function, will be explained below and $\mathcal{Y}_{AB}(E, \omega)$ is a finite-size correction term. It consists of an intrinsic term $\mathcal{Y}^{(1)} = O(L^{-d})$ and an extrinsic term $\mathcal{Y}^{(2)} = O(\Delta^2 E / L^{2d})$ arising from the energy uncertainty. When the energy variance scales as $\Delta^2 E = O(L^d)$ or is smaller than that, we have

$$\mathcal{Y}_{AB}(E, \omega) = O(L^{-d}). \quad (10)$$

The detailed derivation and the explicit expression of \mathcal{Y} are presented in Supplemental Material [40].

Matrix elements $R_{\alpha\gamma}^A$ and $R_{\gamma\alpha}^B$ are random variables, so are their products $R_{\alpha\gamma}^A R_{\gamma\alpha}^B$. The overlap function $\mathcal{R}_{AB}(E, \omega)$ is defined as the mean value of $R_{\alpha\gamma}^A R_{\gamma\alpha}^B$ among all pairs of eigenstates such that $(E_\gamma + E_\alpha)/2 = E$ and $(E_\gamma - E_\alpha)/\hbar = \omega$ within the infinitesimal range [40]:

$$R_{\alpha\gamma}^A R_{\gamma\alpha}^B = \mathcal{R}_{AB}(E = E_{\gamma\alpha}, \omega = \omega_{\gamma\alpha}) + \eta_{\gamma\alpha}^{AB} \quad (11)$$

with a random variable $\eta_{\gamma\alpha}^{AB}$ of zero mean. The overlap function is similar but slightly different from the noise kernel of Ref. [12]. When $\hat{A} = \hat{B}$, it is trivial that $\mathcal{R}_{AA}(E, \omega) = 1$. The overlap function reflects a quantum mechanical correlation between two observables, and is a crucial ingredient for the FDT [12]. Its existence will be verified numerically shortly. For Hermitian operators, $\mathcal{R}_{AB}(E, \omega) = \mathcal{R}_{AB}(E, -\omega)^* = \mathcal{R}_{BA}(E, -\omega)$.

The KMS condition, hence the FDT, can be examined with an indicator function

$$g_{AB}(\omega) = \frac{1}{\hbar\omega} \ln \left[\frac{\bar{S}_{AB}(\omega)}{\bar{S}_{BA}(-\omega)} \right]. \quad (12)$$

When the FDT is valid, the indicator function is independent of ω and equal to the inverse temperature β . The analytic result (9) leads to $g_{AB}(\omega) = \beta + \delta\beta_{AB}(\omega)$ with a deviation from the FDT given by

$$\delta\beta_{AB}(\omega) = \frac{1}{\hbar\omega} (\mathcal{Y}_{AB}(\bar{E}, \omega) - \mathcal{Y}_{BA}(\bar{E}, -\omega)). \quad (13)$$

It vanishes as $\delta\beta_{AB} = O(L^{-d})$ for $\Delta^2 E \leq O(L^d)$ with the system size. Therefore, we conclude that the ETH system obeys the KMS condition, hence the FDT, in the thermodynamic limit.

Numerical test of the FDT and finite size effect— We perform the numerical analysis to verify the FDT and the finite size effect for isolated quantum systems. The indicator function $g_{AB}(\omega)$ in (12) is a useful measure. If the FDT is valid, it should be a constant equal to the inverse temperature. In this work, we focus on the *energy eigenstate* initial state with $\Delta^2 E = 0$.

We study the spin-1/2 XXZ spin model with nearest and next nearest neighbor couplings in the one-dimensional chain of L sites under the periodic boundary condition [15, 16]. The Hamiltonian is given by $\hat{H} = \frac{1}{1+\lambda} \sum_{l=1}^L [\hat{h}_{l,l+1} + \lambda \hat{h}_{l,l+2}]$ with $\hat{h}_{l,m} = -J(\hat{\sigma}_l^+ \hat{\sigma}_m^- + \hat{\sigma}_l^- \hat{\sigma}_m^+ + \frac{\Delta}{2} \hat{\sigma}_l^z \hat{\sigma}_m^z)$ with the Pauli matrices. The system is nonintegrable with nonzero λ . We focus on the subspace in which states have zero magnetization and are invariant under the translation, the spatial inversion, and the spin reversal. The Hamiltonian is diagonalized exactly numerically (see e.g., Ref. [41]). We set $\hbar = 1$ and fix $J = 1$, $\Delta = 1/2$, and $\lambda = 1$ in numerical calculations.

We choose an energy eigenstate $|\alpha_T\rangle$ whose inverse temperature is closest to a target value β_T , and evaluate a coarse-grained $\bar{S}_{AB}(\omega)$ for a set of discretized ω 's in unit of $\Delta\omega = 0.2$ [40]. The indicator function fluctuates from

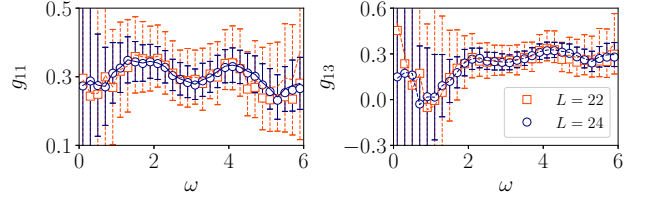


FIG. 1. Mean values (lines) and standard deviations (error bars) of $g_{ij}(\omega)$'s for $\beta_T = 0.3$ at $L = 22$ (dashed) and 24 (solid). The indicator function from the averaged correlation functions is plotted with symbols.

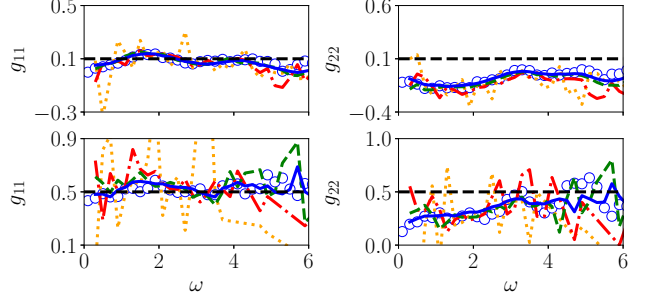


FIG. 2. FDT indicator functions g_{11} for $\hat{A} = \hat{B} = \hat{O}_1$ (left column) and g_{22} for \hat{O}_2 (right column). The target inverse temperatures are $\beta_T = 0.1$ (top) and 0.5 (bottom), which are marked with horizontal lines. The lattice sizes are $L = 18$ (dotted), 20 (dashed dotted), 22 (dashed), and 24 (solid). Predictions from the leading order finite size effect for $L = 24$ are drawn with symbols.

eigenstate to eigenstate. Figure 1 exemplifies the fluctuations of $g_{ij}(\omega)$ for operators $\hat{A} = \hat{O}_i$ and $\hat{B} = \hat{O}_j$ (see next paragraphs for \hat{O}_i). It shows the mean value and the standard deviation of $g_{ij}(\omega)$ among eigenstates $|\alpha\rangle$'s within a window $|E_\alpha - E_T| \leq \frac{\Delta\omega}{2}$ with $\beta_T = 0.3$. The standard deviation decreases by a factor ~ 2 as L increases from 22 to 24, which suggests that the eigenstate-to-eigenstate fluctuations vanish in the thermodynamic limit. Moreover, the mean value is in perfect agreement with the indicator function obtained from the correlation functions averaged within the window. Based on these observations, we will focus on the indicator function calculated from the averaged correlation functions [40].

Firstly, we present the numerical results for single-operator cases $\hat{A} = \hat{B} = \hat{O}_1 \equiv \sum_l \hat{\sigma}_l^z \hat{\sigma}_{l+1}^z$ [nearest neighbor interaction energy] and $\hat{O}_2 \equiv \frac{1}{L} \sum_{l,m} \hat{\sigma}_l^+ \hat{\sigma}_m^-$ [zero momentum distribution]. The indicator functions are shown in Fig. 2. There are noisy fluctuations, which weaken as L increases. For a quantitative analysis, we measure the mean value of the indicator function $g(\omega)$ in the interval $1 < \omega < 5$. It is denoted as β_{FDT} , and plotted as a function of β_T in Fig. 3. For the operator \hat{O}_1 , the plot tends to align with the line $y = x$ as L increases. This may be regarded as a numerical evidence for the FDT. However, the systematic ω dependence of $g(\omega)$ in Fig. 2

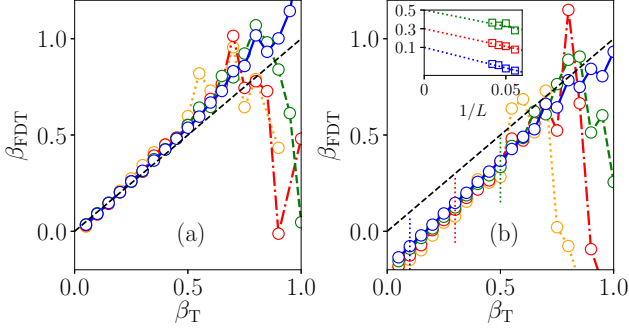


FIG. 3. β_{FDT} vs β_T for $\hat{A} = \hat{B} = \hat{O}_1$ in (a) and \hat{O}_2 in (b). Inset illustrates the $1/L$ dependence of β_{FDT} at $\beta_T = 0.1, 0.3, 0.5$ with lines as guides to eyes.

and a rather conspicuous deviation for \hat{O}_2 in Fig. 3(b) may make the general validity of the FDT questionable.

We also perform the analysis for two-operators cases with $\hat{A} = \hat{O}_1$ and $\hat{B} = \hat{O}_2$ or $\hat{O}_3 \equiv \sum_l (\hat{\sigma}_l^+ \hat{\sigma}_{l+1}^- + \hat{\sigma}_l^- \hat{\sigma}_{l+1}^+)$ [kinetic energy]. We evaluate the FDT indicator functions at the energy eigenstates with $\beta_T = 0.1, 0.3$, and 0.5 . The numerical results for the largest system size $L = 24$ are presented in Fig. 4(a) and (b). The indicator functions exhibit intermittent fluctuations and seem to deviate from β_T significantly. We will show that the apparent deviations observed in Figs. 2 and 3 are indeed the finite size effect.

Our theory predicts that the indicator function should suffer from a finite size effect described by (13). In the energy eigenstate with $\Delta^2 E = 0$, only the intrinsic term $\mathcal{Y}^{(1)}$ contributes to the finite size effect and the deviation from the FDT is given by [40]

$$\delta\beta_{AB}(\omega) = \frac{\partial}{\partial E} \ln [f_A(E, -\omega) f_B(E, \omega) \mathcal{R}_{AB}(E, \omega)]. \quad (14)$$

When $\hat{A} = \hat{B}$, the overlap function $\mathcal{R}_{AA}(E, \omega) = 1$ and the correction term becomes

$$\delta\beta_{AA}(\omega) = \frac{\partial}{\partial E} \ln [f_A(\bar{E}, -\omega) f_A(\bar{E}, \omega)]. \quad (15)$$

The function $f_A(E, \omega)$ determining the fluctuation amplitude of offdiagonal matrix elements in the ETH can be evaluated numerically. We explain our numerical method in Supplemental Material [40]. For $L = 24$, we evaluate $\delta\beta$ in (15) numerically, and compare the indicator function g and thus-obtained $\beta + \delta\beta$ in Fig. 2. The two curves $g(\omega)$ and $\beta + \delta\beta$ are in good agreement.

We also test the finite size effect for $\hat{A} \neq \hat{B}$. The overlap functions are evaluated at the energy values corresponding to the inverse temperature $\beta = 0.1, 0.3$, and 0.5 [40]. They are plotted in Fig. 4(c) and (d). Using the numerical data, we can evaluate the finite size correction term in (14). Figure 4 (a) and (b) show that the indicator function and the finite size correction theory are in excellent agreement. The overlap function $\mathcal{R}_{12}(\omega)$ has zeros,

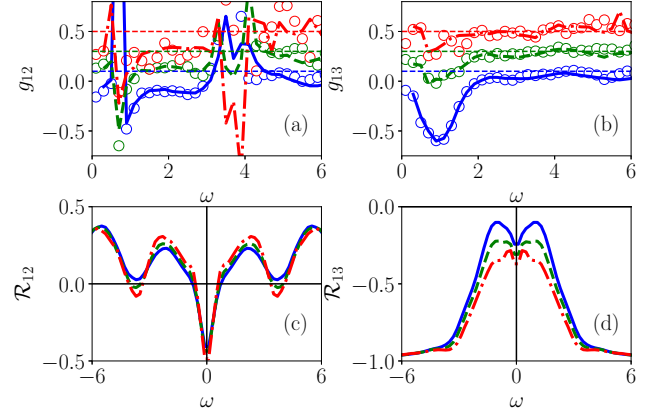


FIG. 4. FDT indicator functions $g_{12}(\omega)$ in (a) and $g_{13}(\omega)$ in (b) for $L = 24$ and $\beta_T = 0.1$ (solid), 0.3 (dashed), 0.5 (dashed dotted). Also shown are the finite size correction form with symbols. The overlap functions $\mathcal{R}_{12}(\omega)$ and $\mathcal{R}_{13}(\omega)$ are shown in (c) and (d) with the same parameter values.

at which the correlation function $\bar{S}_{12}(\omega) \propto \mathcal{R}_{12}(\omega)$ also vanishes. The intermittent fluctuations in $g_{12}(\omega)$ occur near the zeros. $\mathcal{R}_{13}(E, \omega)$ varies more rapidly with β at small values of ω , explains the strong finite size effect for $g_{13}(\omega)$. We have also investigated the FDT, the finite size effect, and the overlap functions for five different observables [40]. We add a remark that the numerical results do not depend on a particular choice of $\Delta\omega$ (see Fig. S4 in [40]).

The function f and \mathcal{R} may scale with the system size L [21, 42]. An overall scale factor, if any, cancels out in taking the logarithmic derivative in (14). Because the derivative is taken with respect to the extensive quantity $E = O(L^d)$, the correction term scales as $\delta\beta_{AB}(\omega) = O(L^{-d})$. The inset of Fig. 3(b) confirms that numerical data are consistent with the finite size scaling $(\beta_{\text{FDT}} - \beta_T) = O(L^{-1})$. Therefore, we conclude that our numerical data confirms the FDT in the infinite size limit.

Discussions and summary— The FDT plays crucial roles in various fields of condensed matter physics, since it can be used to extract information on the response to an external perturbation from equilibrium fluctuations. Our result can serve as a theoretical foundation of the FDT for pure quantum states beyond the conventional setup with the Gibbs states. This is particularly relevant to ultracold atoms, for which the FDT has been experimentally investigated [29, 43]. For example, in Ref. [43], the magnetic susceptibility is obtained from measurements of equilibrium fluctuations. We expect that the FDT is also experimentally useful for temperature measurements of isolated systems, as is numerically confirmed in the present work.

Verifying the FDT experimentally in isolated quantum systems is a challenge. The KMS condition, explained

in this work, can be tested in an experiment with a frequency-resolved measurement of correlation functions. Suppose that the energy variance is negligible. Combining (9) and (14) and eliminating the microscopic overlap function, the finite size correction term $\delta\beta_{AB}$ can be rewritten as

$$\delta\beta_{AB} = -\frac{\hbar\omega}{2} \frac{\partial\beta}{\partial E} + \frac{\partial}{\partial E} \ln \bar{S}_{AB} + O(L^{-2d}), \quad (16)$$

which involves the quantities experimentally accessible. Our theory for the finite size correction will be useful in an experimental study because experimental system sizes available are definitely finite [4, 5].

This work is supported by the National Research Foundation of Korea (NRF) grant funded by the Korea government (MSIP) (Grants No. 2019R1A2C1009628 (JDN) and No. R2017R1D1A09000527 (JY)). TS is supported by JSPS KAKENHI Grant Numbers JP16H02211 and JP19H05796. TS is grateful to Takeshi Fukuhara and Shuta Nakajima for valuable discussions.

-
- [1] Toshiya Kinoshita, Trevor Wenger, and David S Weiss, “A quantum Newton’s cradle,” *Nature* **440**, 900–903 (2006).
 - [2] S Trotzky, Y-A Chen, A Flesch, I P McCulloch, U. Schollwöck, J Eisert, and I Bloch, “Probing the relaxation towards equilibrium in an isolated strongly correlated one-dimensional Bose gas,” *Nat. Phys.* **8**, 325–330 (2012).
 - [3] T Langen, S Erne, R Geiger, B Rauer, T Schweigler, M Kuhnert, W Rohringer, I E Mazets, T Gasenzer, and J Schmiedmayer, “Experimental observation of a generalized Gibbs ensemble,” *Science* **348**, 207–211 (2015).
 - [4] A M Kaufman, M E Tai, A Lukin, M Rispoli, Robert Schittko, Philipp M Preiss, and Markus Greiner, “Quantum thermalization through entanglement in an isolated many-body system,” *Science* **353**, 794–800 (2016).
 - [5] Christian Gross and Immanuel Bloch, “Quantum simulations with ultracold atoms in optical lattices,” *Science* **357**, 995–1001 (2017).
 - [6] Yijun Tang, Wil Kao, Kuan-Yu Li, Sangwon Seo, Krishnanand Mallayya, Marcos Rigol, Sarang Gopalakrishnan, and Benjamin L Lev, “Thermalization near Integrability in a Dipolar Quantum Newton’s Cradle,” *Phys. Rev. X* **8**, 021030 (2018).
 - [7] J M Deutsch, “Quantum statistical mechanics in a closed system,” *Phys. Rev. A* **43**, 2046–2049 (1991).
 - [8] Peter Reimann, “Foundation of Statistical Mechanics under Experimentally Realistic Conditions,” *Phys. Rev. Lett.* **101**, 190403–4 (2008).
 - [9] Anthony J Short, “Equilibration of quantum systems and subsystems,” *New J. Phys.* **13**, 053009–11 (2011).
 - [10] H Wilming, M Goihl, I Roth, and J Eisert, “Entanglement-Ergodic Quantum Systems Equilibrate Exponentially Well,” *Phys. Rev. Lett.* **123**, 200604 (2019).
 - [11] Mark Srednicki, “Thermal fluctuations in quantized chaotic systems,” *J. Phys. A* **29**, L75–L79 (1996).
 - [12] Luca D’Alessio, Yariv Kafri, Anatoli Polkovnikov, and Marcos Rigol, “From quantum chaos and eigenstate thermalization to statistical mechanics and thermodynamics,” *Adv. Phys.* **65**, 239–362 (2016).
 - [13] Joshua M Deutsch, “Eigenstate thermalization hypothesis,” *Rep. Prog. Phys.* **81**, 082001–17 (2018).
 - [14] Marcos Rigol, Vanja Dunjko, and Maxim Olshanii, “Thermalization and its mechanism for generic isolated quantum systems,” *Nature* **452**, 854–858 (2008).
 - [15] Hyungwon Kim, Tatsuhiko N Ikeda, and David A Huse, “Testing whether all eigenstates obey the eigenstate thermalization hypothesis,” *Phys. Rev. E* **90**, 052105 (2014).
 - [16] Toru Yoshizawa, Eiki Iyoda, and Takahiro Sagawa, “Numerical Large Deviation Analysis of the Eigenstate Thermalization Hypothesis,” *Phys. Rev. Lett.* **120**, 200604 (2018).
 - [17] Marcos Rigol, “Breakdown of Thermalization in Finite One-Dimensional Systems,” *Phys. Rev. Lett.* **103**, 015101–4 (2009).
 - [18] R Steinigeweg, J Herbrych, and P Prelovšek, “Eigenstate thermalization within isolated spin-chain systems,” *Phys. Rev. E* **87**, 012118–5 (2013).
 - [19] Rubem Mondaini, Keith R Fratus, Mark Srednicki, and Marcos Rigol, “Eigenstate thermalization in the two-dimensional transverse field Ising model,” *Phys. Rev. E* **93**, 032104–9 (2016).
 - [20] Rubem Mondaini and Marcos Rigol, “Eigenstate thermalization in the two-dimensional transverse field Ising model. II. Off-diagonal matrix elements of observables,” *Phys. Rev. E* **96**, 012157–10 (2017).
 - [21] Marcin Mierzejewski and Lev Vidmar, “Quantitative Impact of Integrals of Motion on the Eigenstate Thermalization Hypothesis,” *Phys. Rev. Lett.* **124**, 040603 (2020).
 - [22] Lea F Santos, Anatoli Polkovnikov, and Marcos Rigol, “Entropy of Isolated Quantum Systems after a Quench,” *Phys. Rev. Lett.* **107**, 040601–4 (2011).
 - [23] Krishnanand Mallayya and Marcos Rigol, “Quantum Quenches and Relaxation Dynamics in the Thermodynamic Limit,” *Phys. Rev. Lett.* **120**, 070603 (2018).
 - [24] S Camalet, “Joule Expansion of a Pure Many-Body State,” *Phys. Rev. Lett.* **100**, 180401 (2008).
 - [25] Jae Dong Noh, Eiki Iyoda, and Takahiro Sagawa, “Heating and cooling of quantum gas by eigenstate Joule expansion,” *Phys. Rev. E* **100**, 010106(R) (2019).
 - [26] Ryogo Kubo, Morikazu Toda, and Natsuki Hashitsume, *Statistical Physics II*, Nonequilibrium Statistical Mechanics, Vol. 31 (Springer, Berlin, 1985).
 - [27] G F Mazenko, *Nonequilibrium Statistical Mechanics* (Wiley-VCH, Weinheim, 2006).
 - [28] J Kurchan, “In and out of equilibrium,” *Nature* **433**, 222–225 (2005).
 - [29] Nathan Gemelke, Xibo Zhang, Chen-Lung Hung, and Cheng Chin, “In situ observation of incompressible Mott-insulating domains in ultracold atomic gases,” *Nature* **460**, 995–998 (2009).
 - [30] Mohammad Mehboudi, Anna Sanpera, and Luis A Correa, “Thermometry in the quantum regime: recent theoretical progress,” *J. Phys. A* **52**, 303001–50 (2019).
 - [31] Laura Foini, Leticia F Cugliandolo, and Andrea Gambassi, “Dynamic correlations, fluctuation-dissipation relations, and effective temperatures after a quantum quench of the transverse field Ising chain,” *J. Stat. Mech.* **2012**, P09011–64 (2012).
 - [32] Laura Foini, Andrea Gambassi, Robert Konik, and Leti-

- cia F Cugliandolo, “Measuring effective temperatures in a generalized Gibbs ensemble,” *Phys. Rev. E* **95**, 247–8 (2017).
- [33] Fabian H L Essler, Stefano Evangelisti, and Maurizio Fagotti, “Dynamical Correlations After a Quantum Quench,” *Phys. Rev. Lett.* **109**, 247206–5 (2012).
- [34] Elliott H Lieb and Derek W Robinson, “The Finite Group Velocity of Quantum Spin Systems,” *Commun. Math. Phys.*, 425–431 (1972).
- [35] Mark Srednicki, “The approach to thermal equilibrium in quantized chaotic systems,” *J. Phys. A* **32**, 1163–1175 (1999).
- [36] Ehsan Khatami, Guido Pupillo, Mark Srednicki, and Marcos Rigol, “Fluctuation-Dissipation Theorem in an Isolated System of Quantum Dipolar Bosons after a Quench,” *Phys. Rev. Lett.* **111**, 050403–5 (2013).
- [37] Charlie Nation and Diego Porras, “Quantum chaotic fluctuation-dissipation theorem: Effective Brownian motion in closed quantum systems,” *Phys. Rev. E* **99**, 052139 (2019).
- [38] R Haag, N M Hugenholtz, and M Winnink, “On the Equilibrium states in quantum statistical mechanics,” *Commun. Math. Phys.* **5**, 215–236 (1967).
- [39] Uwe C Täuber, *Critical Dynamics*, A Field Theory Approach to Equilibrium and Non-Equilibrium Scaling Behaviour (Cambridge University Press, Cambridge, 2014).
- [40] See the Supplemental Materials.
- [41] Jung-Hoon Jung and Jae Dong Noh, “Guide to Exact Diagonalization Study of Quantum Thermalization,” *J. Korean Phys. Soc.* **76**, 670–683 (2020).
- [42] Tyler LeBlond, Krishnanand Mallayya, Lev Vidmar, and Marcos Rigol, “Entanglement and matrix elements of observables in interacting integrable systems,” *Phys. Rev. E* **100**, 1–11 (2019).
- [43] Jakob Meineke, Jean-Philippe Brantut, David Stadler, Torben Müller, Henning Moritz, and Tilman Esslinger, “Interferometric measurement of local spin fluctuations in a quantum gas,” *Nat. Phys.* **8**, 454–458 (2012).
-

Supplemental Materials

Jae Dong Noh¹, Takahiro Sagawa², and Joonhyun Yeo³

¹*Department of Physics, University of Seoul, Seoul 02504, Korea*

²*Department of Applied Physics, The University of Tokyo,
7-3-1 Hongo, Byunkyo-ku, Tokyo 113-8656, Japan*

³*Department of Physics, Konkuk University, Seoul 05029, Korea*

DERIVATION OF THE KMS CONDITION EQ. (3) FROM THE ETH

Applying the ETH to the operators \hat{A} and \hat{B} , one can write

$$\bar{S}_{AB}(\omega) = 2\pi \sum_{\alpha} p_{\alpha} \sum_{\gamma \neq \alpha} e^{-S(E_{\gamma\alpha})} f_A(E_{\alpha\gamma}, \omega_{\alpha\gamma}) f_B(E_{\gamma\alpha}, \omega_{\gamma\alpha}) R_{\alpha\gamma}^A R_{\gamma\alpha}^B \delta(\omega - \omega_{\gamma\alpha}). \quad (\text{S1})$$

The energy eigenvalues are densely distributed for large system sizes. Thus, one can replace \sum_{γ} with $\int dE_{\gamma} D(E_{\gamma})$ with the density of state function $D(E_{\gamma}) = e^{S(E_{\gamma})}$. The individual matrix elements of R^A and R^B are random variables with zero mean and unit variance [11, 12]. On the other hand, $R_{\alpha\gamma}^A$ and $R_{\gamma\alpha}^B$ sharing the same eigenstates may be correlated with a nonvanishing value of $R_{\alpha\gamma}^A R_{\gamma\alpha}^B$ on average. Along the line of the ETH, we make an ansatz that $R_{\alpha\gamma}^A R_{\gamma\alpha}^B$ in (S1) can be replaced by a smooth function $\mathcal{R}_{AB}(E_{\gamma\alpha}, \omega_{\gamma\alpha})$, which will be called the overlap function. It satisfies

$$\mathcal{R}_{AB}(E, \omega) = \mathcal{R}_{AB}(E, -\omega)^* = \mathcal{R}_{BA}(E, -\omega) \quad (\text{S2})$$

for Hermitian operators \hat{A} and \hat{B} . When $\hat{A} = \hat{B}$, $\mathcal{R}_{AA}(E_{\gamma\alpha}, \omega_{\gamma\alpha}) = 2\delta_{\alpha\gamma} + (1 - \delta_{\alpha\gamma})$. Then, the correlation function can be written as

$$\bar{S}_{AB}(\omega) = 2\pi \sum_{\alpha} p_{\alpha} e^{-S(E_{\alpha} + \hbar\omega/2) + S(E_{\alpha} + \hbar\omega)} Q_{AB}(E_{\alpha} + \hbar\omega/2, \omega) \quad (\text{S3})$$

with the auxiliary function

$$Q_{AB}(E, \omega) \equiv f_A(E, -\omega) f_B(E, \omega) \mathcal{R}_{AB}(E, \omega) = Q_{AB}(E, -\omega)^* = Q_{BA}(E, -\omega). \quad (\text{S4})$$

We proceed with small $\delta E_{\alpha} = (E_{\alpha} - \bar{E}) = O(L^{d/2})$ expansion with the mean energy $\bar{E} = \text{Tr} \rho_i \hat{H} = O(L^d)$. The entropy term becomes

$$\begin{aligned} S(E_{\alpha} + \hbar\omega) - S(E_{\alpha} + \hbar\omega/2) &= S(\bar{E} + \delta E_{\alpha} + \hbar\omega) - S(\bar{E} + \delta E_{\alpha} + \hbar\omega/2) \\ &= S(\bar{E} + \hbar\omega) - S(\bar{E} + \hbar\omega/2) + (\delta E_{\alpha}) \{ \partial_E S(\bar{E} + \hbar\omega) - \partial_E S(\bar{E} + \hbar\omega/2) \} \\ &\quad + \frac{1}{2} (\delta E_{\alpha})^2 \{ \partial_E^2 S(\bar{E} + \hbar\omega) - \partial_E^2 S(\bar{E} + \hbar\omega/2) \} + O\left(\frac{(\delta E_{\alpha})^3}{\bar{E}^3}\right). \end{aligned} \quad (\text{S5})$$

On the other hand, we have

$$\begin{aligned} \ln Q_{AB}(E_{\alpha} + \hbar\omega/2, \omega) &= \ln Q_{AB}(\bar{E} + \hbar\omega/2, \omega) + (\delta E_{\alpha}) \partial_E \ln Q_{AB}(\bar{E} + \hbar\omega/2, \omega) \\ &\quad + \frac{1}{2} (\delta E_{\alpha})^2 \partial_E^2 \ln Q_{AB}(\bar{E} + \hbar\omega/2, \omega) + O\left(\frac{(\delta E_{\alpha})^3}{\bar{E}^3}\right). \end{aligned} \quad (\text{S6})$$

We put the above two equations into Eq. (S3) and expand the exponential in powers of δE_{α} . We then reexponentiate it after averaging over the initial distribution given by p_{α} to obtain

$$\begin{aligned} \bar{S}_{AB}(\omega) &= 2\pi \exp \left[S(\bar{E} + \hbar\omega) - S(\bar{E} + \hbar\omega/2) + \ln Q_{AB}(\bar{E} + \hbar\omega/2, \omega) \right. \\ &\quad \left. + \frac{1}{2} \Delta^2 E \left\{ \partial_E S(\bar{E} + \hbar\omega) - \partial_E S(\bar{E} + \hbar\omega/2) + \partial_E \ln Q_{AB}(\bar{E} + \hbar\omega/2, \omega) \right\}^2 \right. \\ &\quad \left. + \frac{1}{2} \Delta^2 E \left\{ \partial_E^2 S(\bar{E} + \hbar\omega) - \partial_E^2 S(\bar{E} + \hbar\omega/2) + \partial_E^2 \ln Q_{AB}(\bar{E} + \hbar\omega/2, \omega) \right\} + O\left(\frac{(\delta E_{\alpha})^3}{\bar{E}^3}\right) \right], \end{aligned} \quad (\text{S7})$$

where $\Delta^2 E \equiv \sum_{\alpha} p_{\alpha} (\delta E_{\alpha})^2$ is the energy variance of the initial state.

Now we note that $\beta = (\partial_{\bar{E}} S)$ is the inverse temperature at the energy \bar{E} in the microcanonical ensemble, which is an intensive quantity. If we expand the quantities in Eq. (S7) around \bar{E} , each derivative with respect to \bar{E} contributes a factor of $O(L^{-d})$. We can therefore write

$$\begin{aligned} \bar{S}_{AB}(\omega) &= 2\pi \exp \left[\frac{\hbar\omega}{2} \beta + \ln Q_{AB}(\bar{E}, \omega) + \left\{ \frac{3(\hbar\omega)^2}{8} (\partial_{\bar{E}} \beta) + \frac{\hbar\omega}{2} \partial_{\bar{E}} \ln Q_{AB}(\bar{E}, \omega) \right\} + O\left(\frac{1}{\bar{E}^2}\right) \right. \\ &\quad \left. + \frac{1}{2} \Delta^2 E \left\{ \left(\frac{\hbar\omega}{2} \partial_{\bar{E}} \beta + \partial_{\bar{E}} \ln Q_{AB}(\bar{E}, \omega) \right)^2 + \frac{\hbar\omega}{2} \partial_{\bar{E}}^2 \beta + \partial_{\bar{E}}^2 \ln Q_{AB}(\bar{E}, \omega) + O\left(\frac{1}{\bar{E}^3}\right) \right\} + O\left(\frac{(\delta E_{\alpha})^3}{\bar{E}^3}\right) \right] \\ &= 2\pi e^{\frac{1}{2}\beta\hbar\omega} Q_{AB}(\bar{E}, \omega) \exp \left[\mathcal{Y}_{AB}(\bar{E}, \omega) + O\left(\max \left\{ \frac{1}{\bar{E}^2}, \frac{\Delta^2 E}{\bar{E}^3}, \frac{(\delta E_{\alpha})^3}{\bar{E}^3} \right\} \right) \right], \end{aligned} \quad (\text{S8})$$

where $\mathcal{Y}_{AB}(E, \omega) = \mathcal{Y}_{AB}^{(1)}(E, \omega) + \mathcal{Y}_{AB}^{(2)}(E, \omega)$ with

$$\mathcal{Y}_{AB}^{(1)}(E, \omega) = \frac{3(\hbar\omega)^2}{8} (\partial_E \beta) + \frac{\hbar\omega}{2} \frac{\partial}{\partial E} \ln Q_{AB}(E, \omega), \quad (\text{S9})$$

$$\mathcal{Y}_{AB}^{(2)}(E, \omega) = \frac{1}{2} \Delta^2 E \left[\frac{(\hbar\omega)^2}{4} (\partial_E \beta)^2 + \frac{\hbar\omega}{2} \partial_E^2 \beta + \hbar\omega (\partial_E \beta) (\partial_E \ln Q_{AB}(E, \omega)) + \frac{\partial_E^2 Q_{AB}(E, \omega)}{Q_{AB}(E, \omega)} \right]. \quad (\text{S10})$$

Notice that $\mathcal{Y}_{AB}^{(1)}$ involves the partial derivative of the scale-independent quantities with respect to the extensive quantity $E = O(L^d)$. Thus, it scales as $\mathcal{Y}^{(1)} = O(L^{-d})$. The second term $\mathcal{Y}_{AB}^{(2)}$ is nonzero only when the initial state has an energy uncertainty with nonzero $\Delta^2 E$. In addition, it involves the partial derivative with respect to the energy twice. Thus, it scales as $\mathcal{Y}_{AB}^{(2)} = O(\Delta^2 E / E^2)$. When $\Delta^2 E = O(L^d)$ as in ordinary noncritical thermal systems, $\mathcal{Y}_{AB}^{(2)}(E, \omega) = O(L^{-d})$. Therefore, in the infinite system size limit, the correction term \mathcal{Y} vanishes and the correlation function becomes $\bar{S}_{AB}(\omega) = 2\pi e^{\frac{1}{2}\beta\hbar\omega} Q_{AB}(\bar{E}, \omega)$, which obeys the KMS condition.

NUMERICAL METHOD FOR \bar{S}_{AB} AND \mathcal{R}_{AB}

In this section, we explain the numerical method to evaluate the correlation function \bar{S}_{AB} and the overlap functions \mathcal{R}_{AB} . As a prerequisite, we assume that the complete set of energy eigenstates $\{|\alpha\rangle\}$ and the matrix elements for \hat{A} and \hat{B} in the energy eigenstate basis are ready.

We will evaluate the correlation function defined in (7) at discrete values of $\omega_n = (n+1/2)\Delta\omega$ with $n = 0, \pm 1, \pm 2, \dots$. It is given by $\bar{S}_{AB}(\omega_n) = \frac{1}{\Delta\omega} \int_{\omega_n - \Delta\omega/2}^{\omega_n + \Delta\omega/2} d\omega \bar{S}_{AB}(\omega)$, and can be evaluated as

$$\bar{S}_{AB}(\omega_n) = \frac{1}{\Delta\omega} \sum_{\alpha} p_{\alpha} \left(\sum_{E_{\alpha} - \Delta\omega/2 < E_{\gamma} < E_{\alpha} + \Delta\omega/2} A_{\alpha\gamma} B_{\gamma\alpha} \right). \quad (\text{S11})$$

If the system is in an energy eigenstate represented by $\hat{\rho}_i = |\alpha_0\rangle \langle \alpha_0|$, then $p_{\alpha} = \delta_{\alpha\alpha_0}$. In the main text, we investigate the correlation function for the energy eigenstate. In order to reduce fluctuations, we choose $p_{\alpha} = \text{constant}$ for $|E_{\alpha} - E_{\alpha_0}| < \Delta\omega/2$ and $p_{\alpha} = 0$ otherwise.

The functions $f_A(E, \omega)$ and $\mathcal{R}_{AB}(E, \omega)$ for $\omega \neq 0$ determine the statistical properties of offdiagonal matrix elements of observables in the energy eigenstate basis in the context of the ETH. We explain our method to evaluate those functions at discrete values of E and ω in units of $\Delta\omega$. We first construct the table $D(E_n)$ for the density of states by counting the number of energy levels $|\alpha\rangle$'s within the interval $E_n - \Delta\omega/2 \leq E_{\alpha} < E_n + \Delta\omega/2$. It is related to the microcanonical ensemble entropy through $D(E_n) = e^{-S(E_n)}$. Then, we separate all pairs of energy eigenstates into discrete sets, each of which is characterized by (E_n, ω_m) and consists of pairs of eigenstates satisfying

$$E_n - \frac{\Delta\omega}{2} \leq E_{\gamma\alpha} \leq E_n + \frac{\Delta\omega}{2} \text{ and } \omega_m - \frac{\Delta\omega}{2} \leq \omega_{\gamma\alpha} < \omega_m + \frac{\Delta\omega}{2}. \quad (\text{S12})$$

It may be helpful to imagine a two-dimensional (E_{α}, E_{γ}) plane as shown in Fig. S1. All pairs of eigenstates characterized by (S12) lie within a cell, which will be denoted as $c_{n,m}$. We remind the readers that $E_{\gamma\alpha} \equiv (E_{\gamma} + E_{\alpha})/2$ and $\omega_{\gamma\alpha} \equiv E_{\gamma} - E_{\alpha}$.

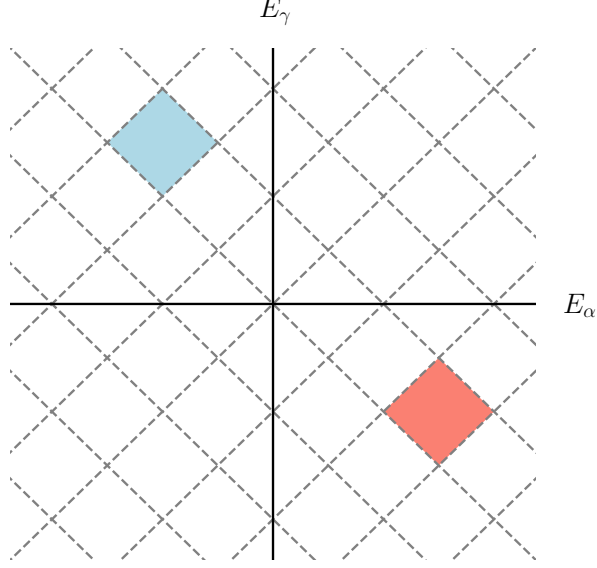


FIG. S1. (E_α, E_γ) plane with meshes for discrete values of $E = (E_\gamma + E_\alpha)/2$ and $\omega = (E_\gamma - E_\alpha)/2$ in unites of $\Delta\omega$. Each cell is represented by the coordinate (E, ω) at the central point. The two shaded cells share the same value of E and have the opposite values of ω .

According to the ETH, an offdiagonal elements of an observable \hat{A} is given by $A_{\gamma\alpha} = e^{-S(E_{\gamma\alpha})/2} f_A(E_{\gamma\alpha}, \omega_{\gamma\alpha}) R_{\gamma\alpha}^A$ where $R_{\gamma\alpha}^A = (R_{\alpha\gamma}^A)^*$ has the same statistical property as the Gaussian random variable with zero mean and unit variance [11]. Using the statistical property of R^A , one can isolate the amplitude of f_A by calculating

$$|f_A(E_n, \omega_m)|^2 = \frac{1}{|c_{n,m}|} \sum_{(E_\alpha, E_\gamma) \in c_{n,m}} D(E_n) A_{\gamma\alpha} A_{\alpha\gamma}, \quad (\text{S13})$$

where $|c_{n,m}|$ is the number of pairs within cell. The factor $D(E_n)$ cancels the entropy factor. The overlap function $\mathcal{R}_{AB}(E_{\gamma\alpha}, \omega_{\gamma\alpha})$ for $R_{\alpha\gamma}^A R_{\gamma\alpha}^B$ can be also constructed by calculating

$$\mathcal{R}_{AB}(E_n, \omega_m) = \frac{1}{|c_{n,m}|} \sum_{(E_\alpha, E_\gamma) \in c_{n,m}} \frac{D(E_n)}{\sqrt{|f_A(E_n, -\omega_m)|^2 |f_B(E_n, \omega_m)|^2}} A_{\alpha\gamma} B_{\gamma\alpha} \quad (\text{S14})$$

Note that $f_A(E, -\omega) = f_A(E, \omega)^*$ and $\mathcal{R}_{AB}(E, -\omega) = \mathcal{R}_{AB}(E, \omega)^*$ for Hermitian operators.

In the numerical study for the XXZ spin chain, we have considered the five different operators:

$$\begin{aligned} \hat{O}_1 &= \sum_l \hat{\sigma}_l^z \hat{\sigma}_{l+1}^z \\ \hat{O}_2 &= \frac{1}{L} \sum_{l,m} \hat{\sigma}_l^+ \hat{\sigma}_m^- \\ \hat{O}_3 &= \sum_l (\hat{\sigma}_l^+ \hat{\sigma}_{l+1}^- + \hat{\sigma}_l^- \hat{\sigma}_{l+1}^+) \\ \hat{O}_4 &= \frac{1}{L} \sum_{l,m} (-1)^{(l-m)} \hat{\sigma}_l^z \hat{\sigma}_m^z \\ \hat{O}_5 &= \frac{1}{L} \sum_{l,m} (-1)^{(l-m)} \hat{\sigma}_l^+ \hat{\sigma}_m^- \end{aligned} \quad (\text{S15})$$

These operators are Hermitian and even under the time reversal. Thus, f_A and \mathcal{R}_{AB} are real valued functions. The three operators \hat{O}_1 , \hat{O}_2 , and \hat{O}_3 are considered in the main text. We evaluate the correlation functions \bar{S}_{AB} for the

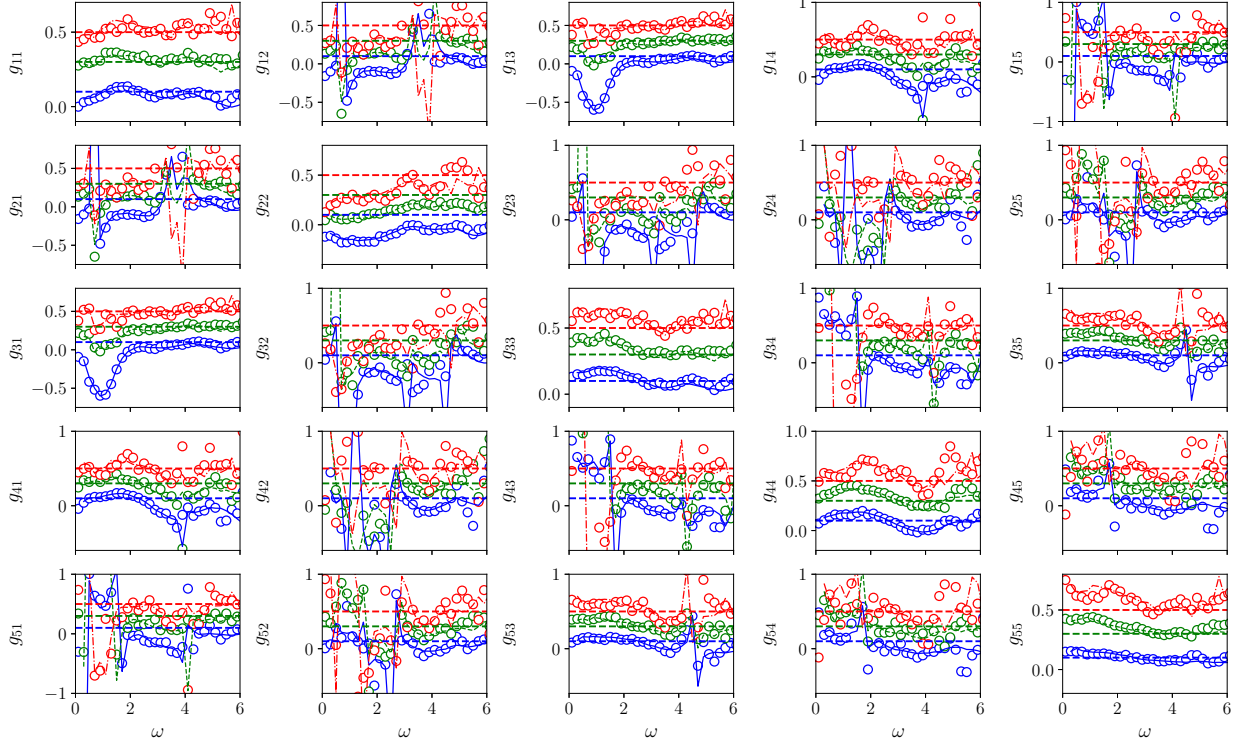


FIG. S2. FDT indicator functions $g_{ij}(\omega)$ (lines) and their finite size correction form (symbols) for the target inverse temperature $\beta = 0.1$ (solid), 0.3 (dashed), and 0.5 (dashed dotted).

operators $\hat{A}, \hat{B} = \hat{O}_i$ using the method explained above, and then calculated the indicator functions $g_{ij}(\omega)$. We take the energy eigenstate $|\alpha_T\rangle$ as the initial state whose inverse temperature is closest to the target values $\beta_T = 0.1, 0.3$, and 0.5 . In order to reduce a statistical fluctuation, we also perform the calculations for the initial states $|\alpha\rangle$ within the energy interval $E_T - \Delta\omega/2 < E_\alpha < E_T + \Delta\omega/2$, and take the average over them. All the numerical data at system size $L = 24$ are plotted in Fig. S2 along with the finite size correction form $\beta = \beta + \delta\beta_{ij}$. In Fig. S3, we also present the plot of $|f_i(\omega)|^2$ and $\mathcal{R}_{ij}(E, \omega)$ as a function of ω at the energy values corresponding to $\beta = 0.1, 0.3$, and 0.5 .

The results do not depend on the coarse-graining scheme with $\Delta\omega < 1.0$. In Fig. S4, we compare the numerical data obtained with $\Delta\omega = 0.1, 0.2$, and 0.5 for the system of size $L = 24$ and of inverse temperature $\beta = 0.3$. All the data sets are hardly distinguishable. The comparison demonstrates that the existence of the overlap function is not an artifact of the coarse-graining with a finite value of $\Delta\omega$.

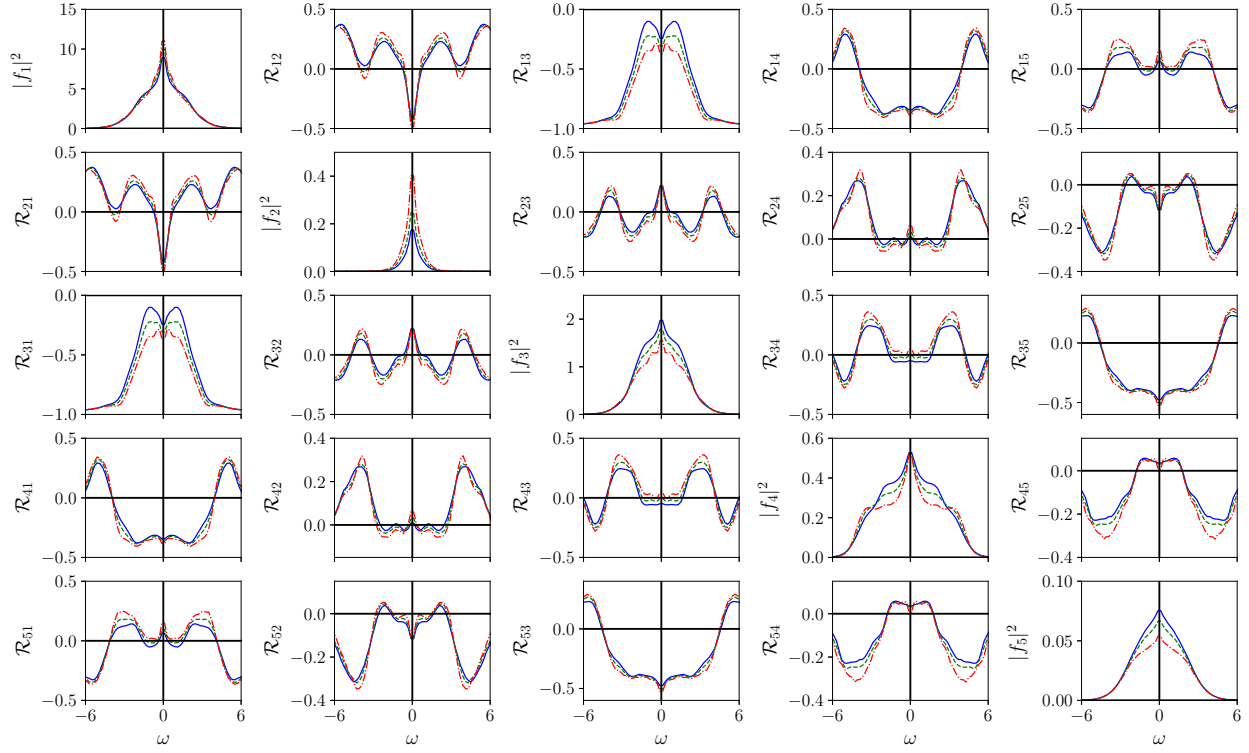


FIG. S3. $|f_i(E, \omega)|^2$ and $\mathcal{R}_{ij}(E, \omega)$ as a function of ω for the operators \hat{O}_i in (S15). The curves are evaluated at the energy value E corresponding to the inverse temperature $\beta = 0.1$ (solid), 0.3 (dashed), and 0.5 (dashed dotted). The diagonal and offdiagonal panels show $|f_i|^2$ and \mathcal{R}_{ij} , respectively.

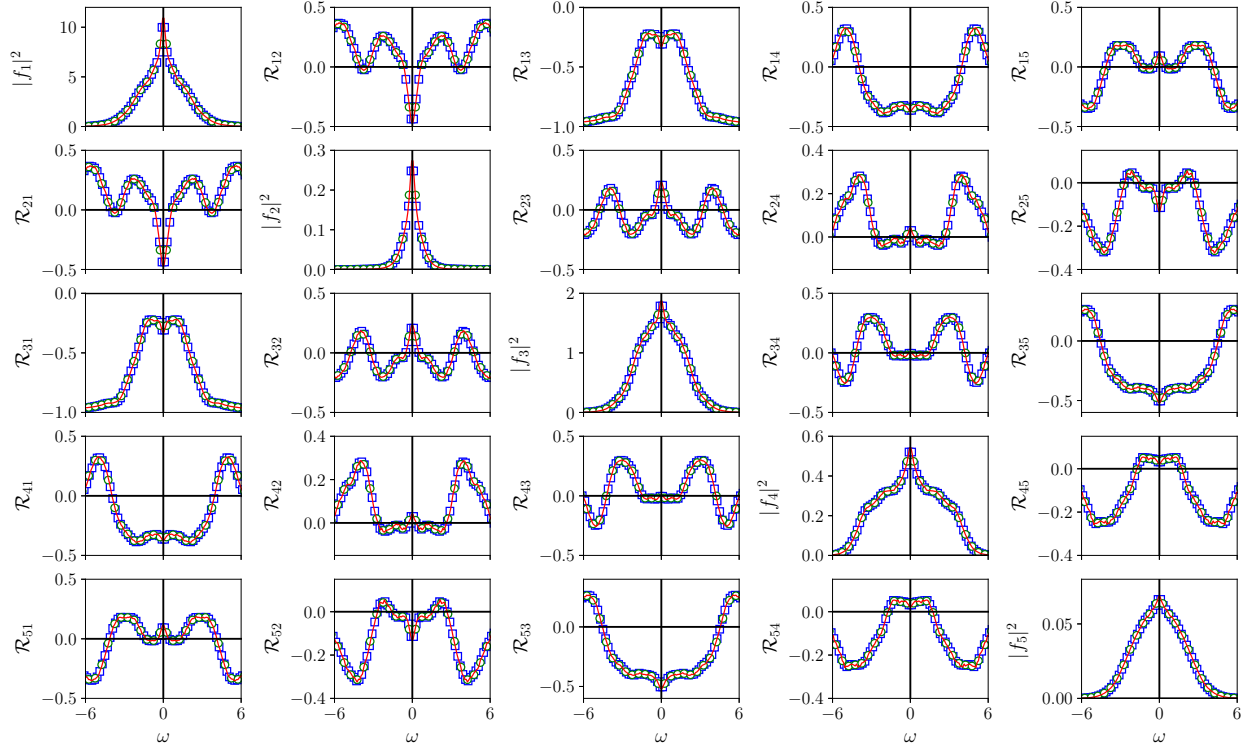


FIG. S4. The same plots as in Fig. S3 with $\beta = 0.3$. The data are obtained with the energy discretization $\Delta\omega = 0.1$ (line), 0.2 (square symbol), and 0.5 (circular symbol).